PHYSICAL REVIEW LETTERS

Evidence for Two Energy Scales in the Superconducting State of Optimally Doped $(Bi, Pb)_2(Sr, La)_2CuO_{6+\delta}$

Takeshi Kondo,[1,2] Tsunehiro Takeuchi,[1,3] Adam Kaminski,[2] Syunsuke Tsuda,[4] and Shik Shin[4]

[1]*Department of Crystalline Materials Science, Nagoya University, Nagoya 464-8603, Japan*
[2]*Ames Laboratory and Department of Physics and Astronomy, Iowa State University, Ames, Iowa 50011, USA*
[3]*EcoTopia Science Institute, Nagoya University, Nagoya 464-8603, Japan*
[4]*Institute of Solid State Physics, University of Tokyo, Kashiwa 277-8581, Japan*
(Received 20 November 2006; published 29 June 2007)

We use angle-resolved photoemission spectroscopy to investigate the energy gap(s) in $(Bi, Pb)_2(Sr, La)_2CuO_{6+\delta}$. We find that the spectral gap has two components in the superconducting state: a superconducting gap and pseudogap. Differences in their momentum and temperature dependence suggest that they represent two separate energy scales. Spectra near the node reveal a sharp peak with a small gap below T_c that closes at T_c. Near the antinode, spectra are broad with a large energy gap of ~ 40 meV above and below T_c. The latter spectral shape and gap magnitude are almost constant across T_c, indicating that the pseudogap state coexists with the superconducting state below T_c, and it dominates spectra around the antinode. We speculate that the pseudogap state competes with the superconductivity by diminishing spectral weight in antinodal regions, where the superconducting gap is largest.

The pseudogap is one of the most fascinating properties of high temperature superconductors [1]. It gives rise to a strange state of matter above T_c where parts of the Fermi surface consist of disconnected "arcs" [2]. Recent angle-resolved photoemission spectroscopy (ARPES) measurements show that the pseudogap state extrapolates at absolute zero to a nodal liquid [3]. Since the pseudogap is often linked to the mechanism of high temperature superconductivity, it is very important to understand its properties and relationship to the superconducting gap. According to one class of theories [4], the pseudogap opens because electrons are paired at temperatures much higher than the critical temperature (T_c) with the same pairing mechanism as the superconducting gap. The pairs only condense below T_c. This scenario is supported by a number of ARPES studies on mostly $Bi_2Sr_2CaC_2O_{8+\delta}$ (Bi2212) suggesting that the behavior and symmetry of the pseudogap above T_c are similar to those of the superconducting gap below T_c [5–7]. Another class of theories [8–10] links the pseudogap to an ordered state with a separate energy scale. The first ARPES experiment designed to detect an ordered state below the pseudogap temperature (T_{PG}) gave a positive result [11]. However, a later ARPES experiment was unable to detect the same small signatures [12]. More recently, a high precision neutron scattering experiment provided direct evidence for the existence of an ordered state with particular symmetry below T_{PG} [13]. This result was consistent with predictions of Varma [9,10] and confirmed the results of the first ARPES study [11]. Recent scanning tunneling microscopy/spectroscopy (STM/STS) experiments on Bi2212 show that even below T_c a pseudogap state, characterized by a large gap and broad spectral peaks, coexists with the superconducting state, which has a smaller energy gap and sharp spectral peaks [14,15]. One drawback of studying the pseudogap in Bi2212 is its large

superconducting gap (~ 40 meV at optimal doping), which is comparable to the pseudogap. We chose to study $(Bi, Pb)_2(Sr, La)_2CuO_{6+\delta}$ (Bi2201), which has a low T_c of ~ 35 K at optimal doping. NMR [16] and electrical resistivity [17] experiments estimate T_{PG} in Bi2201 to be similar to that of Bi2212, while T_c is almost 3 times smaller. Therefore, we should gain an important insight into the relationship between the pseudogap and the superconducting gap by directly measuring the energy gap in Bi2201. In this Letter, we report the momentum and temperature dependence of the energy gap in optimally doped Bi2201 with $T_c = 35$ K. The momentum dependence of the energy gap below T_c strongly deviates from the symmetry of a monotonic $d_{x^2-y^2}$ wave function, which is observed in optimally doped Bi2212 [18]. Our data are most consistent with a two gap component model: a $d_{x^2-y^2}$ wave superconducting gap that dominates the symmetry near the node and a pseudogap that exists only around the antinode.

Optimally doped $(Bi, Pb)_2(Sr, La)_2CuO_{6+\delta}$ ($T_c = 35$ K) single crystals were grown using a conventional floating-zone (FZ) technique [19]. T_c with a sharp transition (~ 3 K) were obtained from electrical resistivity and susceptibility measurements. We substituted Pb for Bi to suppress the modulation in BiO plane, which causes contamination of the ARPES signal from diffraction replicas of the main band. The modulation-free samples enabled us to precisely determine the energy gap. ARPES measurements were made using a Scienta SES2002 hemispherical analyzer with a Gammadata VUV5010 photon source (HeIα) at the Institute of Solid State Physics (ISSP), the University of Tokyo. The energy resolution was 5 meV. The angular resolution was 0.13° and $\sim 0.5°$ along and perpendicular to direction of analyzer slits, respectively.

In Fig. 1, we show the ARPES data [intensity plots and the corresponding energy distribution curves (EDCs)] measured at 7 K well below T_c in the nodal and antinodal regions, respectively. The nodal spectra are characterized by sharp peaks. The leading edge of the EDC at the nodal k_F reaches the Fermi level, indicating there is no energy gap. The spectra at the antinodal cut, in contrast, are very broad. EDCs near the antinodal k_F are shifted towards higher binding energies due to the presence of an energy gap. This effect is illustrated more easily in Figs. 1(c) and 1(f) by use of a symmetrization method [2]; EDCs are reflected about the Fermi level and added to the unreflected ones. This removes the effects of Fermi function and enables us to immediately identify the presence of an energy gap. Clearly, a gap is observed in the data of Fig. 1(f) and is absent in Fig. 1(c).

Figure 2(a) shows the ARPES intensity at the Fermi level. The intensity is strongest near the node and diminishes towards the antinode $(\pi, 0)$. We determined the size of the energy gap using two methods. The first estimates the shift in energy of the midpoint of the EDC leading edge (Δ_{mid}). Figure 2(b) shows the EDCs measured at different k_F for angles ϕ, defined in the inset of Fig. 2(d). The energy gap is zero at the node ($\phi = 45°$), and it increases toward the antinode ($\phi = 0°$). (This method has to be used with caution, because in the absence of the energy gap the midpoint of the leading edge for sharp spectral peaks is located on the positive side of energy axis.) The second method determines the peak position of the symmetrized EDC (Δ_{peak}). Figure 2(c) shows results from this method with the peak positions marked by arrows. Results from both methods are compared in Fig. 2(d). Although the maximum values are different for obvious reasons, both yield a similar symmetry of the gap. A remarkable feature in the momentum dependence of the energy gap is the strong deviation from a monotonic $d_{x^2-y^2}$-wave symmetry,
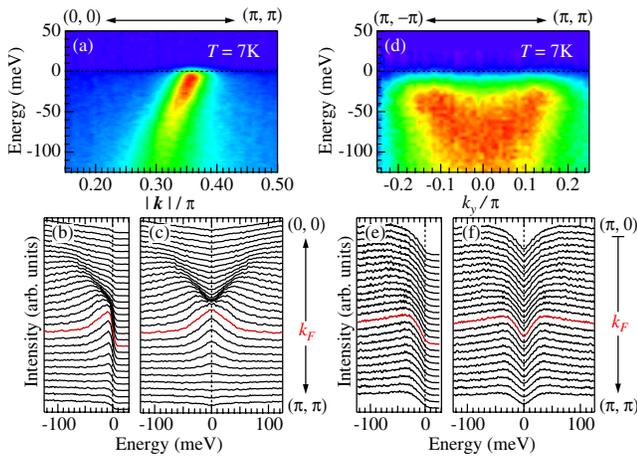
which is illustrated by the dashed line in Fig. 2(d). Harris *et al.* [20] first reported this feature in Bi2201 about a decade ago, and suggested that the enhanced anisotropy is caused by impurity scattering which results in a strong suppression of the energy gap close to the node. The authors measured samples with a large residual resistivity [i.e., small $\rho_{ab}(300\ \text{K})/\rho_{ab}(0\ \text{K})$ ratio of ~2.4], so the idea of an impurity-induced gap symmetry seemed plausible [21]. [Here, ρ_{ab} represents the resistivity along the CuO_2 plane, and $\rho_{ab}(0\ \text{K})$ was estimated from an interpolation to $T = 0$ K.] In this work, we employed high quality single crystals with a much smaller residual resistivity [$\rho_{ab}(300\ \text{K})/\rho_{ab}(0\ \text{K})$ ratio of ~7], yet we observe a similar deviation from the monotonic $d_{x^2-y^2}$-wave symmetry. Hence, impurities are unlikely to be the cause of the characteristic gap symmetry in Bi2201.

It has been reported that the superconducting gap significantly deviates from a monotonic $d_{x^2-y^2}$-wave symmetry in underdoped Bi2212 [22]. This was attributed to an increase of the electron correlation with underdoping, which may increase the intensity of the higher order harmonic component in the d-wave gap function. We fitted a function of the form $\Delta(\phi) = \Delta_0[B \cos(2\phi) + (1 - B) \times \cos(6\phi)]$ to the energy gap in the present data with a
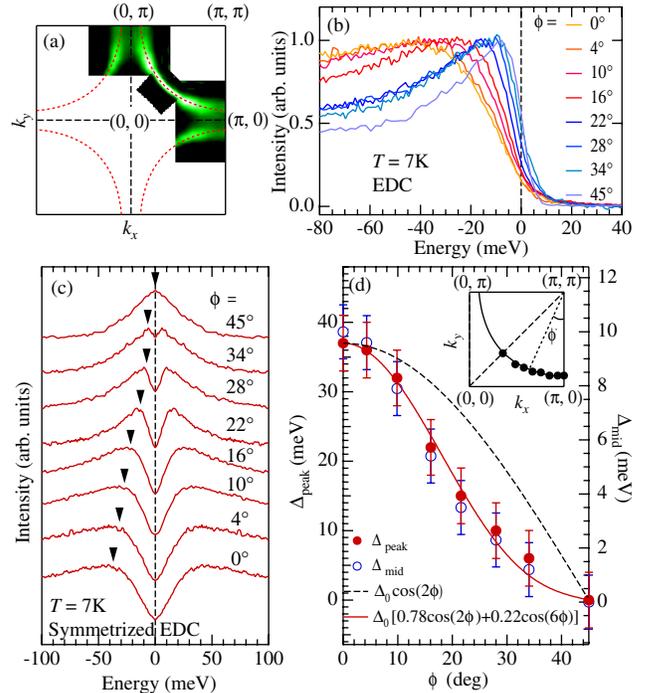
FIG. 2 (color online). (a) ARPES intensity map at the Fermi level. (Spectra normalized at -130 meV.) (b) EDC (normalized to the peak intensity) and (c) symmetrized EDC measured at $T = 7$ K for various k_F's. (d) Magnitude of the energy gap around the Fermi surface at $T = 7$ K (well below T_c) estimated from the midpoint shift of the EDC leading edge (Δ_{mid}) and the peak position in the symmetrized EDC (Δ_{peak}—indicated by the arrows in (c)).

FIG. 1 (color online). ARPES intensity and corresponding EDCs measured at 7 K well below T_c along (a),(b) $(0, 0)-$ (π, π) and (d),(e) $(\pi, -\pi) - (\pi, \pi)$ cut. (c),(f) Symmetrized EDCs of (b),(e).

$\cos(6\phi)$, second order harmonics term in the $d_{x^2-y^2}$ wave. The result is plotted in Fig. 2(d) using a solid line. Even though our Bi2201 samples are optimally doped, we find a much stronger deviation from a pure $d_{x^2-y^2}$ symmetry ($B = 0.78$) compared to underdoped Bi2212 with $T_c = 75$ K ($B = 0.88$) [22]. Hence, the deviation in Bi2201 is unlikely to be due to strong correlation effects.

Figures 3(a)–3(d) show EDCs at four $\boldsymbol{k}_F$'s above and below T_c (7 and 50 K). Spectra near the node [Figs. 3(c) and 3(d)] vary significantly across T_c; the sharp peak below T_c broadens above T_c and the energy gap closes slightly away from the node. This is contrasted by very little variation in the spectral line shape near the antinode across T_c [Figs. 3(a) and 3(b)]. The main feature here is a slight increase in spectral intensity above T_c very close to the Fermi level. The two extreme behaviors evolve rapidly with momentum as evident by comparing 3(f)–3(i) and 3(j)–3(m). They show the ARPES intensity and symmetrized EDCs measured along two momentum cuts crossing $\boldsymbol{k}_F$ at angles $\phi = 16°$ and $28°$, respectively. Above T_c, the gap closes at $\boldsymbol{k}_F$ corresponding to $\phi = 28°$. For $\phi = 16°$ the symmetrized EDC shows a weak variation in the spectral line shape and has an almost unchanged peak position. This generates a large Fermi arc above T_c schematically
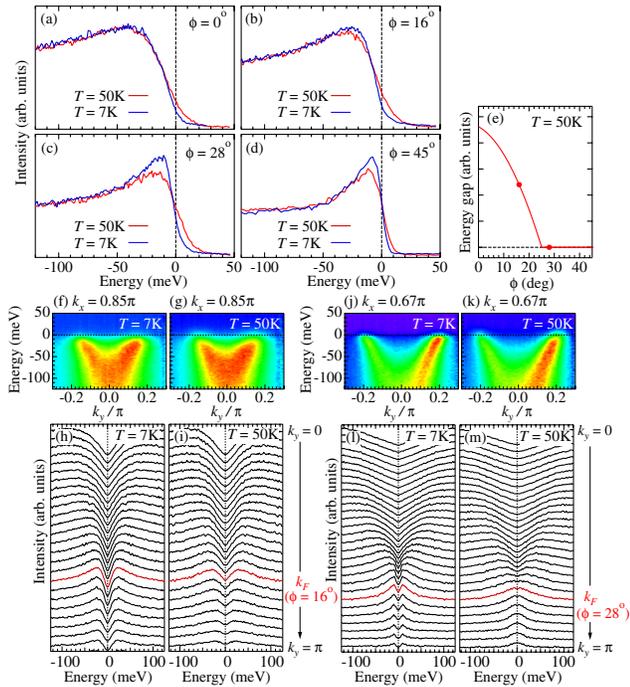
illustrated in Fig. 3(e). Previous results from Bi2212 [2,5] demonstrated that in the pseudogap state the variation of spectral line shape with temperature is quite small. Here we report similar spectral behavior across T_c at antinode with no signature of superconducting transition in the Bi2201. This is contrasted with clear signatures of superconducting gap opening slightly off the nodal point. Absence of dramatic changes that normally accompany the superconducting transition indicates that the energy gap is dominated by the pseudogap even below T_c in the antinodal region.

In order to investigate the pseudogap state, we measured ARPES spectra over a wide temperature range. The resulting symmetrized EDCs are superimposed in Figs. 4(a)–4(d) for several $\boldsymbol{k}_F$'s. The pseudogap is quite large up to 100 K and closes at ~150 K. In optimally doped Bi2212, the pseudogap closing temperature (T_{PG}) has been estimated to be ~130 K by ARPES [23]. Thus the present results indicate that the pseudogap (characterized by the energy gap size and T_{PG}) does not scale with T_c in optimally doped high-T_c cuprates. In Fig. 4(i), we plot the measured energy gap (Δ_{peak}) as a function of angle ϕ at several temperatures ranging from below T_c to above T_{PG}.
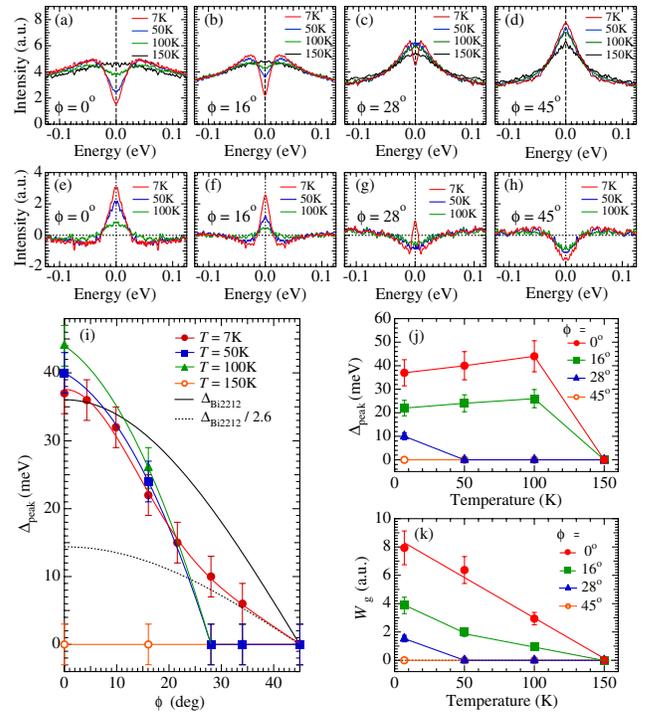

FIG. 3 (color online). (a)–(d) EDC below and above T_c (7 and 50 K) at various $\boldsymbol{k}_F$'s ($\phi = 0°$, $16°$, $28°$, and $45°$). (e) Schematic illustration of energy gap above T_c as a function of the angle ϕ (two solid circles at $\phi = 16°$ and $28°$). ARPES intensity and corresponding symmetrized EDCs measured on a momentum cut at $k_x = 0.85\pi$ crossing $\boldsymbol{k}_F$ of $\phi = 16°$ (f)–(i) and at $k_x = 0.67\pi$ crossing $\boldsymbol{k}_F$ of $\phi = 28°$ (j)–(m). (Contrast of the ARPES intensity between the positive and negative k_y is caused by the matrix element effect).

FIG. 4 (color online). (a)–(d) Symmetrized EDCs at various $\boldsymbol{k}_F$'s ($\phi = 0°$, $16°$, $28°$, and $45°$) and temperatures. (e)–(h) Symmetrized EDC at $T = 150$ K (above the pseudogap closing temperature, T_{PG}) subtracted by one at 7, 50, and 100 K. (i) ϕ dependence of peak position of the symmetrized EDC (Δ_{peak}). Solid black line shows Δ_{peak} for optimally doped Bi2212 [$\Delta_{Bi2212} \propto \cos(2\phi)$] [18,22]. Dashed black line shows Δ_{Bi2212} divided by 2.6 [$\approx T_c(\text{Bi2212})/T_c(\text{Bi2201}) = 90$ K/35 K]. (j) Δ_{peak} and (k) spectral weight lost due to the gap opening (W_g) as a function of temperature.

We also plot the monotonic $d_{x^2-y^2}$-wave function for the superconducting gap of optimally doped Bi2212 [18,22] (solid black line) and that scaled by the ratio of the T_c's in optimally doped Bi2201 and Bi2212 (dashed line). Around the node, the gap at 7 K is consistent with the scaled $d_{x^2-y^2}$-wave gap function. This component disappears above T_c. The energy gap rapidly increases towards the antinode and its maximum value is very similar to that in optimally doped Bi2212. The characteristic gap symmetry below T_c in optimally doped Bi2201, therefore, can be understood as a coexistence of the superconducting state with a small gap (~ 15 meV) that has a monotonic $d_{x^2-y^2}$-wave symmetry and a pseudogap state that has a large energy gap similar to that of optimally doped Bi2212. The former dominates the spectral line shape around the node, while the latter dominates at the antinodal region. In Bi2212, the superconducting gap has a similar energy size to the pseudogap (~ 40 meV at the antinode); thus, these two different gaps are continuously connected across T_c and appear to have the same origin [5,6]. In Bi2201 the superconducting gap is much smaller due to its low T_c, whereas the pseudogap remains large. The very different properties of these two gaps lead us to conclude there is no direct relationship between the pseudogap and the superconducting gap.

Finally, we should comment that while the spectral peak position is a good way to investigate the momentum behavior of the energy gap [Fig. 4(i)], this is not true for the temperature dependence of the pseudogap. We found that, similar to Bi2212 [2,24], the peak position of the symmetrized EDCs around the antinode increases with increasing temperature below the pseudogap closing temperature (T_{PG}) and suddenly jumps to zero above T_{PG}, as illustrated in Fig. 4(j). This is contrasted with the continuous temperature dependence of the spectral shape below T_{PG} [Figs. 4(a)−4(d)]. The peculiar temperature dependence of the pseudogap is illustrated by subtracting the symmetrized EDC below T_{PG} from that above T_{PG} as shown in Figs. 4(e)−4(h). Here we note that when the energy gap is zero as shown at the node [Fig. 4(d)], the difference spectrum has a dip [Fig. 4(h)] due to thermal broadening of the spectral function peak. The difference spectrum has a peak when the energy gap is finite reflecting the loss of spectral weight. We estimated the spectral weight lost when the gap opens (W_G) from the area of the spectral peak in Figs. 4(e)−4(h), and plot it in Fig. 4(k). Near the node, W_{PG} is zero above T_c because the superconducting gap closes. In contrast, W_G around the antinode decreases with increasing temperature in an almost linear fashion up to T_{PG}. The absence of a jump in W_G across T_c strongly suggests that the spectrum around the antinode is dominated by the pseudogap below T_c.

In conclusion, we report momentum and temperature dependence of the energy gap in optimally doped Bi2201 with $T_c = 35$ K. While the superconducting gap, which closes at T_c, is observed around the node, ARPES spectra around the antinode is dominated by the pseudogap state below T_c. Significant differences in the momentum and temperature dependence of the pseudogap and the superconducting gap indicate that there is no direct relationship between the two gaps. We speculate that the pseudogap competes with superconductivity because it diminishes low energy spectral weight around the antinode, where normally the superconducting gap is largest. This is consistent with suppression of superconducting signatures at antinode with decreased doping (increasing pseudogap) as reported by Raman spectroscopy [25,26].

Note added.—After completion of this work, we became aware of related work by Tanaka *et al.* [27].

[1] T. Timusk and B. Statt, Rep. Prog. Phys. **62**, 61 (1999).
[2] M. R. Norman *et al.*, Nature (London) **392**, 157 (1998).
[3] A. Kanigel *et al.*, Nature Phys. **2**, 447 (2006).
[4] V. J. Emery *et al.*, Nature (London) **374**, 434 (1995).
[5] H. Ding *et al.*, Nature (London) **382**, 51 (1996).
[6] A. G. Loeser *et al.*, Science **273**, 325 (1996).
[7] J. C. Campuzano *et al.*, Phys. Rev. Lett. **83**, 3709 (1999).
[8] T. C. Hsu *et al.*, Phys. Rev. B **43**, 2866 (1991).
[9] C. M. Varma, Phys. Rev. B **55**, 14 554 (1997).
[10] C. M. Varma, Phys. Rev. Lett. **83**, 3538 (1999).
[11] A. Kaminski *et al.*, Nature (London) **416**, 610 (2002).
[12] S. V. Borisenko *et al.*, Phys. Rev. Lett. **92**, 207001 (2004).
[13] B. Fauqué *et al.*, Phys. Rev. Lett. **96**, 197001 (2006).
[14] S. H. Pan *et al.*, Nature (London) **413**, 282 (2001).
[15] K. McElroy *et al.*, Phys. Rev. Lett. **94**, 197005 (2005).
[16] Guo-qing Zheng *et al.*, Phys. Rev. Lett. **94**, 047006 (2005).
[17] Yoichi Ando *et al.*, Phys. Rev. Lett. **93**, 267001 (2004).
[18] H. Ding *et al.*, Phys. Rev. B **54**, R9678 (1996).
[19] T. Kondo *et al.*, J. Electron Spectrosc. Relat. Phenom. **137–140**, 663 (2004); Phys. Rev. B **72**, 024533 (2005).
[20] J. M. Harris *et al.*, Phys. Rev. Lett. **79**, 143 (1997).
[21] S. Haas *et al.*, Phys. Rev. B **56**, 5108 (1997).
[22] J. Mesot *et al.*, Phys. Rev. Lett. **83**, 840 (1999).
[23] T. Sato *et al.*, Physica (Amsterdam) **341–348C**, 815 (2000).
[24] M. R. Norman *et al.*, Phys. Rev. B **57**, R11 093 (1998).
[25] M. le Tacon *et al.*, Nature Phys. **2**, 537 (2006).
[26] B. Valenzuela and E. Bascones, Phys. Rev. Lett. **98**, 227002 (2007).
[27] K. Tanaka *et al.*, Science **314**, 1910 (2006).